MATHEMATICAL CHARACTERIZATION OF FRICTIONAL PROPERTIES

by

DANIEL B. HERMANN, B.A.

A THESIS

IN

MATHEMATICS

Submitted to the Graduate Faculty
of Texas Tech University in
Partial Fulfillment of
the Requirements for
the Degree of

MASTER OF SCIENCE

Approved

_____

Co-Chairperson of the Committee

_____

Co-Chairperson of the Committee

_____

Accepted

_____

Dean of the Graduate School

August, 2003

ACKNOWLEDGMENTS

I would like to thank Dr. Padmanabhan Seshaiyer for his support and guidance during our two long years working on my thesis, as well as, his patience at times. I would also like to thank Dr. Seshadri Ramkumar for his guidance and ideas, without which, there would be no thesis to write. I am also very grateful to Dr. Robert Byerly for joining my committee so late and with seemingly few reservations. Thanks are also owed to Dr. Jo Ann Temple for helping out in any way she could.

It has been a difficult last few years, and just for being there when needed and giving me a push when I thought I would give up, I must thank Shawna Allen, Harold Hardy, and Shankha Iqbal. Without them, I might be living at my parents' house right now and wondering what might have been. Finally, I need to thank my parents, Dan and Mary Hermann. They are responsible for who I am today, and they have encouraged me throughout my life to succeed at whatever I do.

CONTENTS

ABSTRACT

Determination of a friction law that describes well the behavior exhibited by a polymeric textile, even under limited conditions, is very challenging. Most of the friction laws presented in the literature for polymers are based directly on experimental data. However, textile materials have been known to deviate from standard friction laws that is used in practice. To quantify a textile material's behavior completely, one has to combine mathematical theory with experimental data. Hence, the focus of this work is to develop a methodology to mathematically characterize the frictional properties of polymeric textiles using experimental data.

LIST OF TABLES

LIST OF FIGURES

CHAPTER I
INTRODUCTION

Most recently, a major upsurge in the research on the frictional characterization of polymeric textiles has taken place primarily due to the need for a standardized friction testing method [1, 2, 3, 4, 5, 6, 7]. Friction has been widely studied by scientists and experimentalists for a long time and the importance of friction to the overall quality and the mechanical properties of solid polymers and textiles has been well researched and documented [8, 9, 10]. Briscoe and Tabor have emphasized the relationship between the friction and wear properties to the bulk properties of polymers [8]. Peirce stressed the importance of friction to the overall quality or the "hand" of fabric but he did not endeavor to experimentally measure the frictional properties [10].

In 1699, Guillaume Amontons proposed a simple linear law of friction, which is $F = \mu \cdot N$, where F is the frictional force, μ is the coefficient of friction, and N is the normal force. However, textile materials have been known to deviate from this law of friction [11, 12, 13, 14]. Experimental research has shown that the friction force-normal load relationship is not a simple linear relationship [3, 4]. Bowden and Tabor proposed a power law of friction given by $F = CN^n$ where C and n are constants [15].

In general, a friction law should describe the gross behavior of a polymeric material, which results from its internal constitution, in response to applied loads. However, it is unreasonable to expect any friction law to describe well all behaviors exhibited by a polymeric material under all conditions. Most of the friction laws presented in the literature for polymers are based directly on experimental data. Strictly speaking, any friction law should be considered valid only for the precise conditions under which it was derived. To quantify a textile material's behavior completely, therefore, one has to combine mathematical theory with experimental data. Theory restricts the possible forms the friction laws can assume and guides the performance and interpretation of the experiments. Experiments provide information on the specific form of the friction law as well as for finding the material parameter values. Hence, the

motivation of the thesis is to develop a methodology to mathematically characterize the frictional properties of polymeric textiles using experimental data.

The outline of this work is as follows. In Chapter II, we present three mathematical models that are based on the most widely used power-law model, and analyze them. In Chapter III, we present the experimental setup for evaluating the material properties. Chapter IV considers the results of applying the three mathematical models (discussed in Chapter II) to the experimental data obtained from the experimental evaluation (presented in Chapter III), as well as presenting visualization tools using two MATLAB Graphical User Interfaces (GUIs) for characterizing frictional properties. Finally, Chapter V offers conclusions and possible future work in the field.

CHAPTER II

MODELING FRICTIONAL PROPERTIES

In this chapter, we present different mathematical models to characterize the friction of polymeric materials. These models are based on the power law model. However, we wish to consider forces to vary depending on the apparent area of contact, A. Thus, the friction force-normal load relationship can be conveniently represented using the equation:

$$F_i/A = C(N_i/A)^n \qquad i = 1, \ldots, m \tag{2.1}$$

where, F_i: friction forces in *Newtons*;

N_i: normal loads in *Newtons*;

A: apparent area in m^2;

C: friction parameter in $Pascal^{1-n}$;

n: friction index (non-dimensional); and

m: number of experimental observations.

Finally, we present a general problem-solving methodology to estimate the friction parameters C and n, given experimental data for F_i/A and N_i/A.

2.1 Linear Model

The first model merely results from developing a linear representation for (2.1). By taking the base 10 logarithm of this equation, we obtain the following linear equation;

$$\log(F_i/A) = \log C + n \log(N_i/A). \tag{2.2}$$

Now we wish to find C and n so that the linear relationship

$$\begin{pmatrix} Y_1 \\ Y_2 \\ \vdots \\ Y_m \end{pmatrix} = \begin{pmatrix} 1 & \log(N_1/A) \\ 1 & \log(N_2/A) \\ \vdots & \vdots \\ 1 & \log(N_m/A) \end{pmatrix} \begin{pmatrix} \log C \\ n \end{pmatrix} \longrightarrow \vec{Y} = B\vec{\alpha}$$

produces $Y_i = \log(F_i/A)$. This is an over-determined system of linear equations for unknown quantities $\log C$ and n, and hence, the system cannot be satisfied exactly for any $\log C$ and n. Since $\text{rank}(B) \leq 2$ and often in practice $m > 2$, the system is more likely to be inconsistent, that is, have no solution. An arbitrary choice of $\log C$ and n would give an error of size

$$|\log(F_i/A) - Y_i|$$

for each i, and trying to satisfy the system approximately implies a compromise with a residual error. Let us denote this error by e_L defined as

$$e_L = \sum_{i=1}^{m} (\log(F_i/A) - Y_i)^2,$$

or

$$e_L = \sum_{i=1}^{m} (\log(F_i/A) - \log C - n \log(N_i/A))^2. \tag{2.3}$$

Our objective then, is to find the solutions $\log C$ and n that minimize e_L. This is given by the following theorem. For simplicity, let us define

$$\bar{N} = \frac{1}{m} \sum_{i=1}^{m} \log(N_i/A) \quad \textit{and} \quad \bar{F} = \frac{1}{m} \sum_{i=1}^{m} \log(F_i/A).$$

Theorem 2.1.1. *The residual error, e_L, is minimized by the solution*

$$n = \frac{\sum_{i=1}^{m} (\log(N_i/A) - \bar{N})(\log(F_i/A) - \bar{F})}{\sum_{i=1}^{m} (\log(N_i/A) - \bar{N})^2} \tag{2.4}$$

$$\log C = \bar{F} - \bar{N} n. \tag{2.5}$$

Proof. The minimum values for e_L can be found by solving

$$\frac{\partial e_L}{\partial \log C} = 0 \quad \text{and} \quad \frac{\partial e_L}{\partial n} = 0,$$

since e_L is quadratic in $\log C$ and n. The equations, then are

$$\begin{aligned} (-2) \sum_i (\log(F_i/A) - \log C - n \log(N_i/A)) &= 0, \\ (-2) \sum_i \log(N_i/A)(\log(F_i/A) - \log C - n \log(N_i/A)) &= 0, \end{aligned}$$

that is,

$$m \log C + n \sum_i \log(N_i/A) = \sum_i \log(F_i/A), \tag{2.6}$$

$$\log C \sum_i \log(N_i/A) + n \sum_i [\log(N_i/A)]^2 = \sum_i \log(N_i/A) \log(F_i/A). \tag{2.7}$$

Now by defining

$$\vec{N} = \begin{pmatrix} \log(N_1/A) \\ \log(N_2/A) \\ \vdots \\ \log(N_m/A) \end{pmatrix}, \quad \textit{and} \quad \vec{F} = \begin{pmatrix} \log(F_1/A) \\ \log(F_2/A) \\ \vdots \\ \log(F_m/A) \end{pmatrix},$$

we can rewrite (2.6) and (2.7) as

$$B^\top B \vec{\alpha} = B^\top \vec{F}. \tag{2.8}$$

Solving this system requires that

$$\det(B^\top B) \neq 0,$$

which is true if two or more components of $\vec{F}$ are distinct, but the data sets used depend on varying the normal loads, and experimental research shows clearly that (2.1) is an increasing monotonic function, so this condition is met. From (2.6), we have,

$$m \log C + nm\bar{N} = m\bar{F}$$

which proves (2.5). We can then rewrite (2.7) as,

$$\bar{N} m \log C + n \sum_i [\log(N_i/A)]^2 = \sum_i \log(N_i/A) \log(F_i/A).$$

Using (2.5) in the above equation yields,

$$
\begin{aligned}
n &= \frac{\sum_i \log(N_i/A)\log(F_i/A) - \bar{F}\bar{N}m}{\sum_i [\log(N_i/A)]^2 - \bar{N}^2 m} \\
&= \frac{\sum_i \log(N_i/A)\log(F_i/A) - \bar{F}\bar{N}m - \bar{F}\bar{N}m + \bar{F}\bar{N}m}{\sum_i [\log(N_i/A)]^2 + \bar{N}^2 m - 2\bar{N}^2 m} \\
&= \frac{\sum_{i=1}^{m} \log(N_i/A)\log(F_i/A) - \bar{F}\sum_{i=1}^{m}\log(N_i/A) - \bar{N}\sum_{i=1}^{m}\log(F_i/A) + \sum_{i=1}^{m}\bar{F}\bar{N}}{\sum_{i=1}^{m}[\log(N_i/A)]^2 + \sum_{i=1}^{m}\bar{N}^2 - 2\sum_{i=1}^{m}\log(N_i/A)\bar{N}} \\
&= \frac{\sum_{i=1}^{m}[\log(N_i/A) - \bar{N}][\log(F_i/A) - \bar{F}]}{\sum_{i=1}^{m}[\log(N_i/A) - \bar{N}]^2}
\end{aligned}
$$

which proves (2.4).

Now it remains to be shown that the solution set (2.4)-(2.5)is a minimum, rather than a saddle point. This can be checked with the second derivatives. Thus we must consider the following:

$$
\begin{aligned}
\frac{\partial^2 e_L}{\partial(\log C)^2} &= 2m, \\
\frac{\partial^2 e_L}{\partial n^2} &= 2\sum_i (\log(N_i/A))^2, \\
\frac{\partial^2 e_L}{\partial(\log C)\partial n} &= \frac{\partial^2 e_L}{\partial n \partial(\log C)} = 2\sum_i \log(N_i/A).
\end{aligned}
$$

From the Cauchy-Schwartz inequality (see Appendix A.1), the discriminant is negative since

$$
\left(\frac{\partial^2 e_L}{\partial n \partial(\log C)}\right)^2 - \left(\frac{\partial^2 e_L}{\partial(\log C)^2}\right)\left(\frac{\partial^2 e_L}{\partial n^2}\right) =
$$

$$
4\left[\left(\sum_i \log(N_i/A)\right)^2 - m\sum_i (\log(N_i/A))^2\right] < 0,
$$

whenever

$$\det(B^{\top}B) \neq 0,$$

and both

$$\frac{\partial^2 e_L}{\partial(\log C)^2} > 0 \quad \text{and} \quad \frac{\partial^2 e_L}{\partial n^2} > 0$$

as at least two components of $\vec{N}$ are distinct. Therefore the solutions for $\log C$ and n indeed form a minimum. □

Remark 2.1.1. *The advantage of this model is that it is the simplest one to use. However, the major disadvantage is that if the data does not follow a linear pattern, the error for this model could be relatively large.*

2.2 Quasi-Linear Model

The second model is similar to the linear model, but it assumes an error, initially. We wish

$$F_i/A \approx C(N_i/A)^n.$$

So define ϵ_i such that

$$F_i/A - C(N_i/A)^n = \epsilon_i, \tag{2.9}$$

where ϵ_i is an initial error for each observation. Rewriting (2.9), we have

$$F_i/A - \epsilon_i = C(N_i/A)^n.$$

Taking the base 10 logarithm yields

$$\log(F_i/A - \epsilon_i) = \log(C(N_i/A)^n),$$

which can be simplified to give,

$$\log(F_i/A) + \log\left(1 - \frac{\epsilon_i}{F_i/A}\right) = \log(C(N_i/A)^n). \tag{2.10}$$

The Taylor polynomial approximation (see Appendix A.2) of the function $\log(1-x)$ about $x = 0$ yields

$$\log(1-x) \sim \log(1-x)|_{x=0} - \frac{1}{1-x}|_{x=0}(x-0) + \frac{1}{(1-x)^2}\frac{(x-0)^2}{2} \ldots .$$

The linear approximation gives,

$$\log(1-x) \sim -x. \tag{2.11}$$

Applying this approximation with $x = \frac{\epsilon_i}{(F_i/A)}$ to (2.10) gives

$$\log(F_i/A) - \frac{\epsilon_i}{(F_i/A)} = \log(C(N_i/A)^n).$$

Solve for ϵ_i to get

$$\epsilon_i = (F_i/A)(\log(F_i/A) - \log(C(N_i/A)^n)). \tag{2.12}$$

We can then define

$$e_{QL} = \sum_i \epsilon_i^2 = \sum_i (F_i/A)^2(\log(F_i/A) - (\log C + n\log(N_i/A)))^2,$$

or

$$e_{QL} = \sum_i (F_i/A)^2(\log(F_i/A) - \log C - n\log(N_i/A))^2. \tag{2.13}$$

So, as with the linear model, for the quasi-linear model to be useful, values for $\log C$ and n must be determined so that e_{QL} is minimum. This is given by the following theorem.

Theorem 2.2.1. *The residual error, e_{QL}, is minimized by the solutions*

$$n = \frac{S}{T} \tag{2.14}$$

$$\log C = \frac{\sum_{i=1}^{m}(F_i/A)^2\log(F_i/A) - n\sum_{i=1}^{m}(F_i/A)^2\log(N_i/A)}{\sum_{i=1}^{m}(F_i/A)^2} \tag{2.15}$$

where

$$S = \left(\sum_{i=1}^{m}(F_i/A)^2\right)\left(\sum_{i=1}^{m}(F_i/A)^2\log(N_i/A)\log(F_i/A)\right) - \left(\sum_{i=1}^{m}(F_i/A)^2\log(F_i/A)\right)\left(\sum_{i=1}^{m}(F_i/A)^2\log(N_i/A)\right)$$

and

$$T = \left(\sum_{i=1}^{m}(F_i/A)^2\right)\left(\sum_{i=1}^{m}(F_i/A)^2(\log(N_i/A))^2\right) - \left[\sum_{i=1}^{m}(F_i/A)^2\log(N_i/A)\right]^2.$$

Proof. The minimum values for e_{QL} can be found by solving

$$\frac{\partial e_{QL}}{\partial \log C} = 0 \quad \text{and} \quad \frac{\partial e_{QL}}{\partial n} = 0,$$

since e is quadratic in $\log C$ and n. The equations, then are

$$\begin{aligned}(-2)\sum_i[(F_i/A)^2(\log(F_i/A) - \log C - n\log(N_i/A))] &= 0,\\ (-2)\sum_i[(F_i/A)^2\log(N_i/A)(\log(F_i/A) - \log C - n\log(N_i/A))] &= 0,\end{aligned}$$

that is,

$$\begin{aligned}\log C\sum_i(F_i/A)^2 + n\sum_i[(F_i/A)^2\log(N_i/A)] &= \sum_i[(F_i/A)^2\log(F_i/A)], \qquad (2.16)\\ \log C\sum_i[(F_i/A)^2\log(N_i/A)] + n\sum_i[(F_i/A)^2[\log(N_i/A)]^2] &= \sum_i[(F_i/A)^2\log(N_i/A)\log(F_i/A)]. \qquad (2.17)\end{aligned}$$

Now by defining

$$D = \begin{pmatrix} F_1/A & (F_1/A)\log(N_1/A)\\ F_2/A & (F_2/A)\log(N_2/A)\\ \vdots & \vdots\\ F_m/A & (F_m/A)\log N_m/A \end{pmatrix},$$

$$\vec{N} = \begin{pmatrix} (F_1/A)\log(N_1/A) \\ (F_2/A)\log(N_2/A) \\ \vdots \\ (F_m/A)\log(N_m/A) \end{pmatrix}, \text{ and } \quad \vec{F} = \begin{pmatrix} (F_1/A)\log(F_1/A) \\ (F_2/A)\log(F_2/A) \\ \vdots \\ (F_m/A)\log(F_m/A) \end{pmatrix},$$

we can rewrite 2.16 and 2.17 as

$$D^\top D\vec{\alpha} = D^\top \vec{F}. \tag{2.18}$$

Solving this system requires that

$$\det(D^\top D) \neq 0,$$

which is true if two or more components of $\vec{F}$ are distinct, but, as was explained in developing the linear model, (2.1) is an increasing monotonic function, so this condition is met. From (2.16) we can solve for $\log C$ to have (2.15). Using (2.15) we can then rewrite (2.17) as

$$\frac{\sum_{i=1}^{m}(F_i/A)^2\log(F_i/A) - n\sum_{i=1}^{m}(F_i/A)^2\log(N_i/A)}{\sum_{i=1}^{m}(F_i/A)^2}\sum_{i=1}^{m}(F_i/A)^2\log(N_i/A) +$$

$$n\sum_{i=1}^{m}(F_i/A)^2(\log(N_i/A))^2 = \sum_{i=1}^{m}(F_i/A)^2\log(N_i/A)\log(F_i/A),$$

which when we solve for n, we obtain (2.14).

Now it remains to be shown that the solution set (2.14)-(2.15) is a minimum, rather than a saddle point. This can be checked with the second derivatives. Thus we must consider the following.

$$\begin{aligned} \frac{\partial^2 e_{QL}}{\partial(\log C)^2} &= 2\sum_i (F_i/A)^2, \\ \frac{\partial^2 e_{QL}}{\partial n^2} &= 2\sum_i [(F_i/A)^2(\log(N_i/A))^2], \\ \frac{\partial^2 e_{QL}}{\partial(\log C)\partial n} &= \frac{\partial^2 e_{QL}}{\partial n\partial(\log C)} = 2\sum_i [(F_i/A)^2\log(N_i/A)]. \end{aligned}$$

From the Cauchy-Schwartz inequality, the discriminant is negative since

$$\left(\frac{\partial^2 e_{\mathrm{QL}}}{\partial n \partial(\log C)}\right)^2 - \left(\frac{\partial^2 e_{\mathrm{QL}}}{\partial(\log C)^2}\right)\left(\frac{\partial^2 e_{\mathrm{QL}}}{\partial n^2}\right) =$$

$$4\left[\left(\sum_i [(F_i/A)^2 \log(N_i/A)]\right)^2 - \sum_i (F_i/A)^2 \sum_i [(F_i/A)^2 \log(N_i/A)]^2\right] < 0,$$

whenever

$$\det(D^\top D) \neq 0,$$

and both

$$\frac{\partial^2 e_{\mathrm{QL}}}{\partial(\log C)^2} > 0 \quad \text{and} \quad \frac{\partial^2 e_{\mathrm{QL}}}{\partial n^2} > 0$$

as at least two N_i/As are distinct. Therefore the solutions for $\log C$ and n form a minimum. □

2.3 Non-Linear Model

The non-linear is, in essence, the direct approach. The goal for this model is to consider working directly with (2.1). In other words, we wish to find C and n so that

$$e_{\mathrm{NL}} = \sum_i (F_i/A - C(N_i/A)^n)^2 \tag{2.19}$$

is minimum. Now, in order to find C and n where e_{NL} is minimum, we need to solve

$$\frac{\partial e_{\mathrm{NL}}}{\partial C} = 0 \quad \text{and} \quad \frac{\partial e_{\mathrm{NL}}}{\partial n} = 0.$$

So the following system must be solve:

$$\begin{cases} \dfrac{\partial e_{\mathrm{NL}}}{\partial C} = \displaystyle\sum_i (2C(N_i/A)^{2n} - 2(N_i/A)^n (F_i/A)) = 0, \\ \dfrac{\partial e_{\mathrm{NL}}}{\partial n} = \displaystyle\sum_i (C^2 (N_i/A)^{2n} \ln N_i/A - 2C(N_i/A)^n (F_i/A)\ln(N_i/A)) = 0. \end{cases}$$

Now, as in the linear case, it is necessary to check that the above solution set does define a minimum for the problem. However, in the linear model, the partial derivatives are linear with respect to their variables, $\log C$ and n, while in the non-linear model, the system is one of non-linear partial derivatives with respect to the variables

C and n. In order to handle this problem we will apply Newton's method for solving a system of non-linear equations. Let us suppose (C_1, n_1) is an approximate solution to the non-linear system. Then it would be appropriate to compute corrections h_1 and h_2 so that $(C_1 + h_1, n_1 + h_2)$ is a better approximate solution. Now using only linear terms of the Taylor expansion in two variables (see Appendix A.3) we get the new system

$$\begin{aligned} \frac{\partial e_{\mathrm{NL}}}{\partial C}(C_1 + h_1, n_1 + h_2) &\approx e_1 + h_1 \frac{\partial^2 e_{\mathrm{NL}}}{\partial C^2}(C_1, n_1) + h_2 \frac{\partial^2 e_{\mathrm{NL}}}{\partial C \partial n}(C_1, n_1) \;=\; 0, \\ \frac{\partial e_{\mathrm{NL}}}{\partial n}(C_1 + h_1, n_1 + h_2) &\approx e_2 + h_1 \frac{\partial^2 e_{\mathrm{NL}}}{\partial n \partial C}(C_1, n_1) + h_2 \frac{\partial^2 e_{\mathrm{NL}}}{\partial n^2}(C_1, n_1) \;=\; 0, \end{aligned} \tag{2.20}$$

where

$$e_1 = \frac{\partial e_{\mathrm{NL}}}{\partial C}(C_1, n_1) \quad \text{and} \quad e_2 = \frac{\partial e_{\mathrm{NL}}}{\partial n}(C_1, n_1).$$

Now the system is a linear system in terms of h_1 and h_2. We can rewrite (2.20) as,

$$J\vec{h} = -\vec{e} \tag{2.21}$$

where

$$J = \begin{pmatrix} \dfrac{\partial^2 e_{\mathrm{NL}}}{\partial C^2} & \dfrac{\partial^2 e_{\mathrm{NL}}}{\partial C \partial n} \\ \\ \dfrac{\partial^2 e_{\mathrm{NL}}}{\partial n \partial C} & \dfrac{\partial^2 e_{\mathrm{NL}}}{\partial n^2} \end{pmatrix} \quad \vec{h} = \begin{pmatrix} h_1 \\ h_2 \end{pmatrix} \quad \vec{e} = \begin{pmatrix} e_1 \\ e_2 \end{pmatrix}.$$

If J is nonsingular the solution is given by,

$$\vec{h} = -J^{-1}\vec{e}.$$

Thus, Newton's method for two non-linear equations in two variables becomes the recursive formula

$$\begin{pmatrix} C_1^{(k+1)} \\ n_1^{(k+1)} \end{pmatrix} = \begin{pmatrix} C_1^{(k)} \\ n_1^{(k)} \end{pmatrix} + \begin{pmatrix} h_1^{(k)} \\ h_2^{(k)} \end{pmatrix}$$

where $C_1^{(k)}$ is the kth approximation for C, and where the Jacobian linear system (2.21) is solved by Gaussian elimination.

2.4 Methodology for Characterizing Frictional Properties

In this section, we present a general problem-solving methodology to characterize the frictional properties of polymers.

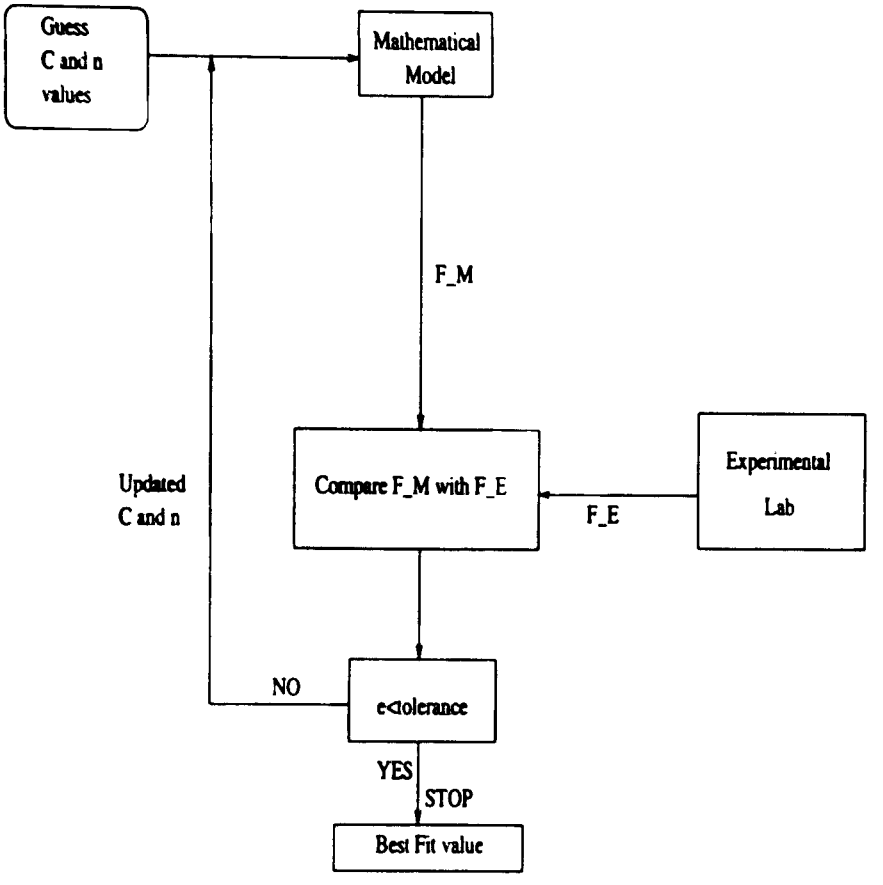

Figure 2.1: Flowchart illustrating a general methodology to determine frictional properties. F_M denotes computed (or mathematical) friction force and F_E denotes experimental friction force.

For a given configuration, as well as, initial guess for the values of the material parameters, an appropriate mathematical model calculates a candidate solution and hence the calculated quantity of interest $\vec{F_M}$ (which may be the frictional forces). For the same configuration, one can also measure the frictional forces (for various normal loads), which can be denoted by $\vec{F_E}$. Then the values of $\vec{F_M}$ and $\vec{F_E}$ are compared via a least-squares regression method to assess the accuracy of the solution from the mathematical model. If the error in the regression is within the prescribed tolerance,

then the most recently guessed parameter values are accepted as the best-fit values. If not, this procedure continues iteratively until acceptable estimates are found for the frictional properties. Hence, the methodology simply requires multiple forward model solutions based on updated "guesses" for the parameters from the regression algorithm. This is illustrated by the flowchart in Figure 2.1.

CHAPTER III
EXPERIMENTAL EVALUATION OF FRICTIONAL PROPERTIES

It is known that the frictional properties of textile materials depend on a number of testing parameters such as the applied normal load, area of testing, speed of testing, and the nature of the contacting surfaces [11, 14, 16, 17, 18, 19, 20]. There is a a plethora of literature on the influence of applied normal loads and the area of testing. However, there is a paucity of information available on the influence of testing speeds on the frictional properties of textile materials. Nishimatsu and Sawaki have studied the effect of sliding speeds on the frictional property of pile fabrics and have observed a marginal decrease in the friction of fabrics with increase in the velocity of testing [14]. Studies by Ajayi [17] and Virto and Naik [21] have shown that there is limited influence of the sliding speeds on the frictional properties. Most recently, Ramkumar et al. [22] have studied the effects of sliding speeds on the frictional properties of nonwoven fabrics. Results indicated that frictional resistance increased with an increase in the speed of testing. As is evident from the aforementioned discussions, it is clear that the frictional properties of textile materials have to be investigated over a range of applied normal loads and at different speeds of testing.

In this chapter we briefly discuss the experimental setup developed to determine frictional parameters.

3.1 Friction Measurement

A sliding friction apparatus, as shown in Figure 3.1, has been used to measure the frictional forces over a range of applied normal loads. The sliding friction apparatus was attached to a constant rate of extension tensile tester. The sliding friction apparatus consists of an aluminum platform on to which a frictionless pulley is attached. The maximum capacity of the load cell of the tensile tester was 25 kgf. The friction apparatus makes use of a sled having an apparent contact area of 20 cm^2, consisting

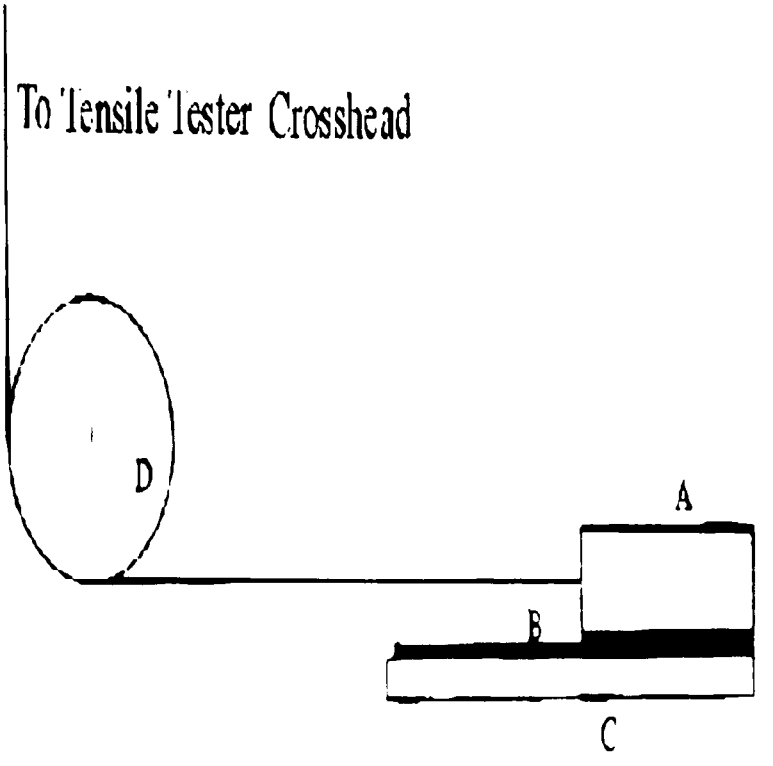

Figure 3.1: Schematic of the sliding friction apparatus where A: PMMA sled; B: fabric; C: aluminum platform; and D: frictionless pulley.

of a polymethyl methacrylate, or PMMA, plate 10 mm in thickness mounted on a wooden block. One end of the sled was attached to the crosshead of the tensile tester by means of a nylon thread through a frictionless pulley as shown in Figure 3.1. Friction testing was carried out at six different applied normal loads. The minimum load used was 39.58 gms and the maximum load used was 89.58 gms. The load was incremented in steps of 10 grams. A rectangular piece of fabric was attached on the horizontal surface of the aluminum platform by a strip of double-sided adhesive tape. Special care was taken in ensuring no wrinkled samples were used, and that while attaching the sample to the tape no excessive pressure was applied. The sled, with the PMMA surface in direct contact with the fabric, was pulled across the sample, and the frictional data was recorded. For this study, the sled was always drawn across the weft, or filling, of the sample. Each test consisted of running the sled across the

fabric using each of the six applied normal loads. Each test consisted of six runs corresponding to each normal applied load for a specified velocity. Five such tests were conducted at each of the five velocities: 250 mm/min, 400 mm/min, 600 mm/min, 750 mm/min, and 1000 mm/min.

Information about the type of fabric used is presented in Table 3.1.

Table 3.1: Details of the fabric used.

Type	100% Cotton (Woven)
Ends/inch	98
Picks/inch	81
Warp count	38.3 Ne
Weft count	37.9 Ne
Weave	Plain (1×1)
Weight	3.32 oz/sq.yd

3.2 Data Collection and Friction Calculation

Both static and dynamic frictional resistance was measured for each run of a normal load for each test, by the Microsoft program Wintest. The program measures the average static and average dynamic friction for each test run.

CHAPTER IV
NUMERICAL RESULTS

In this chapter, we present some numerical results using actual experimental data generated via the setup described in Chapter III. First, we present results on the effect of different applied normal load levels, for the three models developed in Chapter II. Finally, two in-house MATLAB Graphical User Interfaces, or GUIs, that have been developed, are discussed.

4.1 Results of Experimental Evaluation

The intent of the experimental research was to validate the statement that for a particular polymer material, the ratio, $R = C/n$, is constant relative to speed of testing. Matlab programs (see Appendix C) were written to obtain the results appearing in Figures 4.1, 4.2, 4.3, and 4.4. By applying a linear fit to the data from the Wintest program mentioned above, the Matlab program obtained C and n values, and subsequently values for the ratio R. The experimental data was collected for five different speeds using the sliding friction apparatus with PMMA (see Appendix B) as a standard sled. Figure 4.1 indicates that using a linear fit to interpret the experimental data is valid. This is evident from the residuals computed between the experimental and calculated values of frictional resistance. It was observed that the numerical fit was very good for dynamic friction. It can also be noted that static friction can be linearly fitted with relatively good accuracy.

Experiments were run for five different speeds, and the corresponding values of R were computed. Figure 4.2 illustrates the variation in C and n with respect to velocity for the linear model discussed in Section 2.1. Figure 4.3 illustrates the variation in C and n with respect to velocity for the quasi-linear model discussed in Section 2.2. Figure 4.4 illustrates the variation in C and n with respect to velocity for the non-linear model discussed in Section 2.3. Each figure plots the computed static friction (solid lines), experimental static friction (circles), computed dynamic friction (dotted

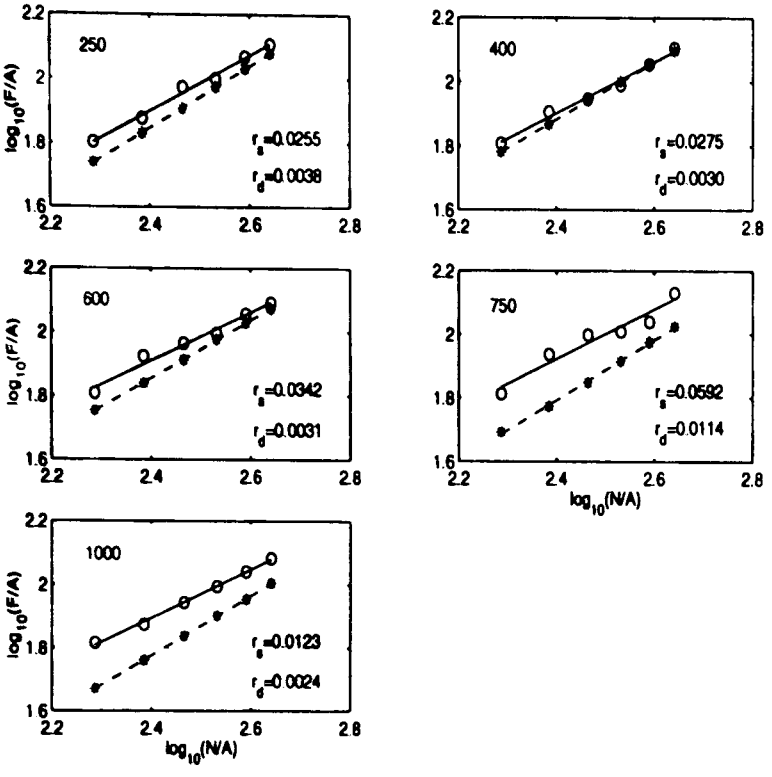

Figure 4.1: $\log_{10}$(Normal load) (N/A) versus $\log_{10}$(frictional resistance) (F/A) for static experimental (circles), static computed (solid lines), dynamic experimental (asterisk), and dynamic computed (dashed line) frictions for cotton fabrics. Here r_s and r_d denote the respective residual error between the computed and experimental values.

lines), and the experimental dynamic friction (asterisks). In fact, testing shows that both C and n are relatively constant in the case of dynamic friction as predicted by our hypothesis. Both the static and dynamic cases are presented. The values of C and n displayed have been calculated for Figure 4.2 using (2.4)-(2.5), Figure 4.3 using (2.14)-(2.15), and Figure 4.4 using (2.19). It has also been observed that the values for the dynamic friction were close in magnitude for every velocity tested. (Figures 4.2, 4.3, and 4.4).

4.2 A MATLAB GUI Implementation for Characterizing Frictional Properties

In this section, we present two new visualization softwares that has been developed using the MATLAB Graphical User Interface (GUI). This tool illustrates how a given

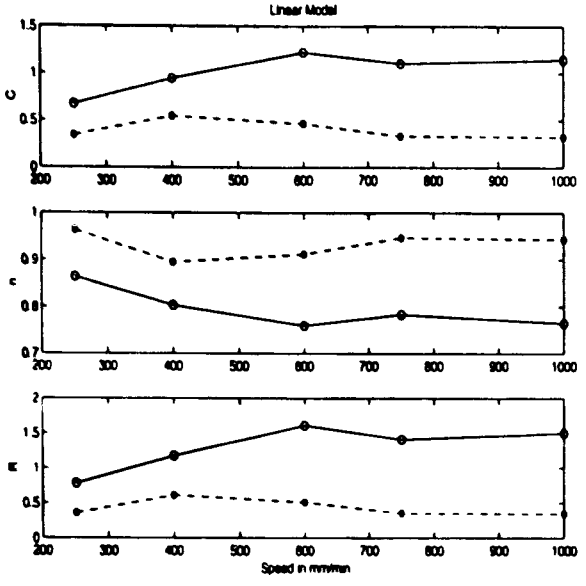

Figure 4.2: Linear Model: Relationship between C, n, and R with respect to velocity.

mathematical model fits the observed experimental data. It allows the user to input frictional forces and normal loads, which are then used to determine appropriate C and n values for (2.1). After doing so, the GUI plots the best-fit equation against the experimental data.

4.2.1 A Simple GUI for the Linear Model

The first software uses the linear model to find C and n for (2.2), and then plots the base 10 logarithms of the data against (2.2). Figure 4.5 indicates the initial screen after running the software without any further actions.

Once the initial screen has appeared, the user may enter normal loads and frictional forces at the bottom of the screen. After doing so, it is important to press the "initialize" push button before plotting. This allows the program to read in the data and compute the necessary values before a plot is considered. After initializing, press the "Linear" push button, and the software will plot the base 10 logarithms of the user's data on the same graph as equation (2.2). The program will require that the

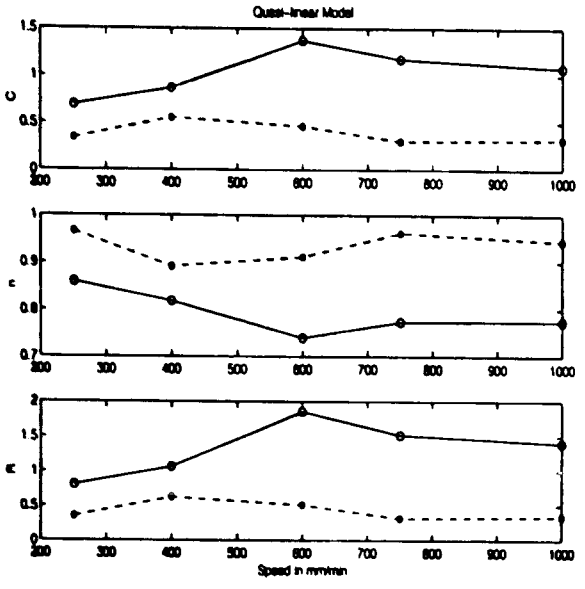

Figure 4.3: Quasi-linear Model: Relationship between C, n, and R with respect to velocity.

user click any location on the graph to place the resulting C and n values. Figure 4.6 depicts the end result after all of the above steps have been followed.

4.2.2 An Advanced GUI for Multiple Models

The second software uses each of the three models in Chapter II to compute C and n values for user-inputted data. Upon initially running this software, the user will see Figure 4.7. This screen will look much like the initial screen for the first software, however, at the top of the screen, there are now "Quasi-Linear" and "Non-Linear" push buttons, besides the "Linear" push button. If the user follows the remaining steps for the first software (linear only), the result will be Figure 4.8. In this software, equation (2.1) is plotted against the actual user-input data (that is, F_i/A versus N_i/A rather than their base 10 logarithms). Repeating the process with the quasi-linear and non-linear buttons, yields the final screen as shown in Figure 4.9. It should be noted that for both softwares presented here, the "initialize" push button must always be pressed after entering new normal loads and frictional forces. Otherwise, the GUI may not graph the desired values.

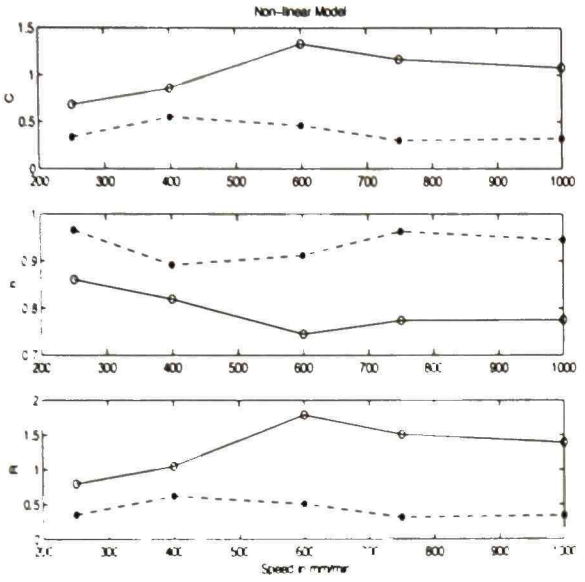

Figure 4.4: Non-linear Model: Relationship between C, n, and R with respect to velocity.

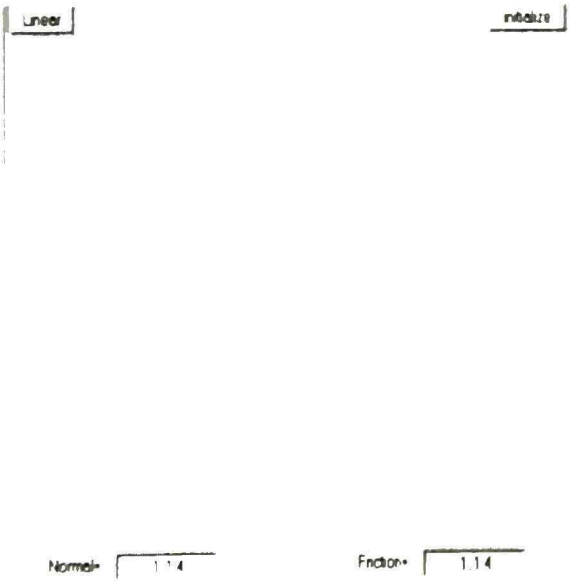

Figure 4.5: Initial screen of a simple GUI for the linear model.

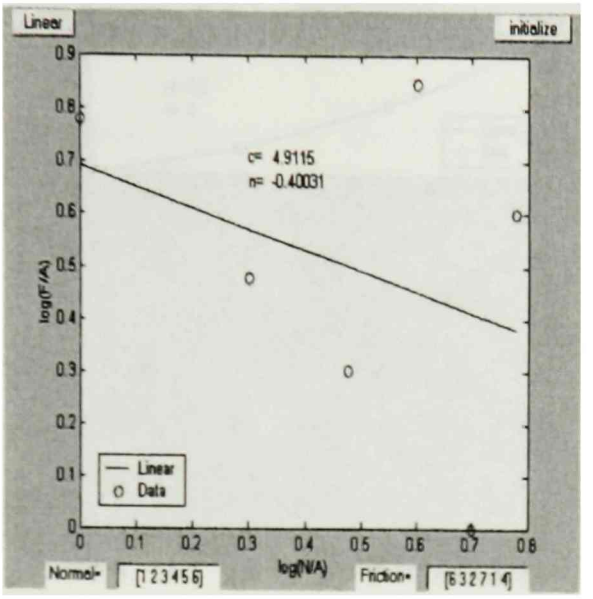

Figure 4.6: Final screen of a simple GUI for the linear model.

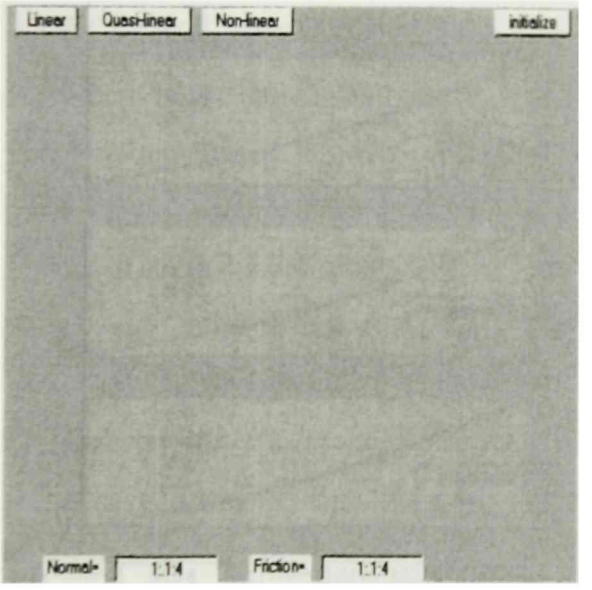

Figure 4.7: Initial screen of an advanced GUI for multiple models.

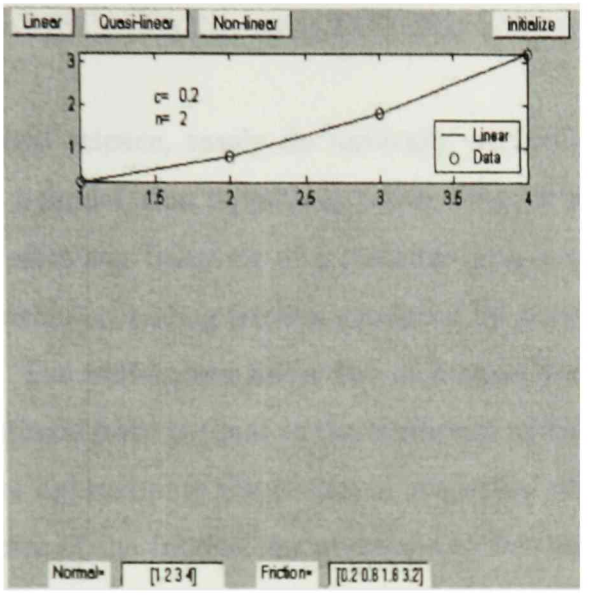

Figure 4.8: Screen of an advanced GUI for multiple models after plotting the linear model.

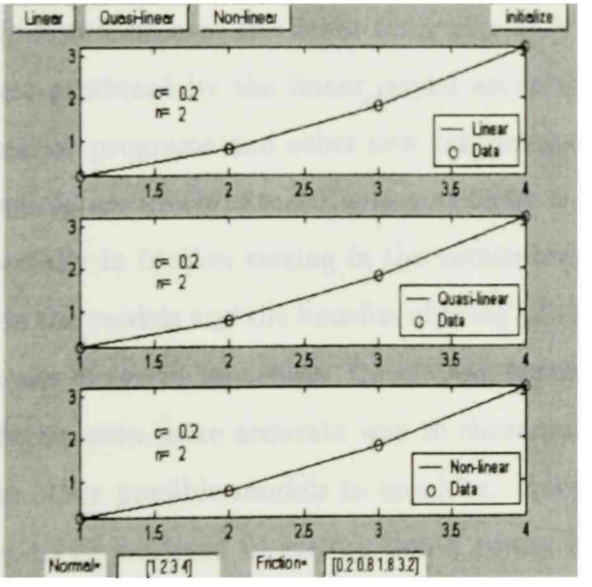

Figure 4.9: Final screen of an advanced GUI for multiple models.

CHAPTER V
CONCLUSIONS AND FUTURE WORK

Throughout physical science, rarely do naturally occurring phenomena appear which fit perfectly to a model, that is, with error=0. Thus, it is necessary to develop models which can predict any behavior of a material with a relatively small degree of error. The phenomenon of sliding friction produced by polymeric materials is not an exception to this. The well-known linear law of friction developed by Amontons, which states that frictional force is equal to the coefficient of friction, μ, multiplied by the normal force, does approximate the frictional properties of polymers to a certain extent. The power form of the friction law presented in this thesis

$$F/A = C(N/A)^n$$

even becomes Amontons' common law if $n = 1$, thus making $C = \mu$. However, research presented in this thesis show the power form produces better accuracy when n has a value nearer to 0.9 (with the appropriate C value). In the past, the added difficulties of using a power form over the linear form may have been too wieldy, thus making the extra error produced by the linear model acceptable. With the advent of mathematical computer programs and other new technologies, the difficulties produced by the power model are much reduced, and now there is greater need for more accurate models, especially in friction testing in the textile industry.

Further research on the models and the benefits of using (2.1) may aid in characterizing frictional properties of textile materials. Developing hybrid models as presented in this thesis may offer an even more accurate way to characterize friction in fabrics, and may even lead to other possible models to consider. Another aspect of this research that may need to be explored in greater detail comes from the experimental values. Notice in Figures 4.2, 4.3, and 4.4 that based on the experimental data obtained during this thesis, values for C appear to increase near 500 mm/min, while values for n appear to decline in the same speed range. Outside of this range, values

for both C and n are approximately constant. Thus, it may be worthwhile to analyze the frictional properties at speeds near 500 mm/min in greater depth.

BIBLIOGRAPHY

[1] Ramkumar, S. S., Leaf, G. A. V., and Harlock, S. C., "A Study of the Frictional Properties of 1×1 Rib-knitted Cotton Fabrics," *J. Text. Inst.*, 91, 2000, 374-382.

[2] Ramkumar, S. S., "Frictional Characterization of Enzyme Treated Fabrics Using a Simple Friction Factor," *AATCC Review*, 2(11), 2002, 24-27.

[3] Ramkumar, S. S., "Tribology of Textile Materials," *Indian J. Fiber and Textile Res.*, 25, 2000, 238.

[4] Ramkumar, S. S., "Method for Determining the Frictional Properties of Materials," *U.S. Patent 6397672*, 2002.

[5] Ramkumar, S. S., Wood, D. J., Fox, K., and Harlock, S. C., "Development of a Polymereic Human Finger Sensor for Studying the Frictional Properties of Textiles, Part I: Artificial Finger Development," *Textile Res. J.*, 73(6), 2003, 469.

[6] Ramkumar, S. S., Wood, D. J., Fox, K., and Harlock, S. C., "Development of a Polymereic Human Finger Sensor for Studying the Frictional Properties of Textiles, Part II: Experimental Results," *Textile Res. J.*, July 2003.

[7] Rodel, C. and Ramkumar, S. S., "Surface Mechanical Property Measurements of H1 Technology Needlepunched Nonwovens," *Textile Res. J.*, 73(5), 2003, 381.

[8] Briscoe, B. J. and Tabor, D., "Friction and Wear of Polymers: The Role of Mechanical Properties," *Br. Polym. J.*, 10, 1978, 74-78.

[9] Harlock, S. C. and Ramkumar, S. S., "A Study of the Handle Characteristics of Cotton Rib Knitted Fabrics," in *Textiles and the Information Society (Proceedings of the 78th World Conference of the Textile Institute)*, The Textile Institute, Manchester, Vol. III, 1997, 149-161.

[10] Peirce, F. T., "The Handle of Cloth as a Measurable Quantity," *J. Text. Inst.*, 21, 1930, T377-T416.

[11] Wilson, D., "A Study of Fabric-on-fabric Dynamic Friction," *J. Text. Inst.*, 54, 1963, T143-T155.

[12] Howell, H. G., "Inter-fibre Friction," *J. Text. Inst.*, 42, 1951, T521-T533.

[13] Howell, H. G. and Mazur, J., "Amontons' Law and Fibre Friction," *J. Text. Inst.*, 44, 1953, T59-T69.

[14] Ohsawa, M. and Namiki, S., "Anisotropy of the Static Friction of Plain-woven Filament Fabrics," *J. Text. Mach. Soc. Japan*, 19, 1966, T7-T16 (*Eng. Edn.* 12, 143).

[15] Bowden, T. and Tabor, D., *The Friction and Lubrication of Solids*. Oxford: Oxford University Press, 1950.

[16] Ramkumar, S. S., Shastri, L., Tock, R. W., Shelly, D. C., Smith, M. L., and Padmanabhan, S., "Experimental Study of the Frictional Properties of Friction Sun Yarns," *J. Appl. Polym. Sci.*, 88(10), 2003, 2450-2454.

[17] Ajayi, J. O., "Fabric Smoothness, Friction, and Handle," *Text. Res. J.*, 62, 1992, 52-59.

[18] Dreby, E. C., "A Friction Meter for Determining the Coefficient of Kinetic Friction of Fabrics," *J. Res. Nat. Bur. Stand.*, 31, 1943, 237-246.

[19] Carr, W. W., Posey, J. E., and Tincher, W. C., "Frictional Characteristics of Apparel Fabrics," *Text. Res. J.*, 58, 1988, 129-136.

[20] Clapp, T. G., Timble, N. B., and Gupta, B. S., "Frictional Behaviour of Textile Fabrics," *J. Appl. Polym. Sci.*, 47, 1991, 373-382.

[21] Virto, L. and Naik, A., "Frictional Behavior of Textile Fabrics, Part I: Sliding Phenomena of Fabrics on Metallic and Polymeric Solid Surfaces," *Textile Res. J.*, 67, 1997, 793-802.

[22] Ramkumar, S. S., Umrani, A. S., Parameswaran, S., Shelly, D. C., Tock, R. W., and Smith, M. L., "Study of the Effect of Sliding Velocity on the Frictional Properties of Nonwoven Substrates," *Wear*, (in print).

APPENDIX A

MATHEMATICAL PRELIMINARIES

A.1 Cauchy-Schwarz Inequality

Cauchy-Schwarz inequality. *For any* $x, y \in R^n$ *we have*

$$\sum_{j=1}^{n} |x_j y_j| \leq ||\mathbf{x}||_2 ||\mathbf{y}||_2.$$

Proof. (i) we only need to consider $\mathbf{x} \neq \mathbf{0}$ and $\mathbf{y} \neq \mathbf{0}$, as otherwise the result is trivially $0 = 0$;

(ii) We claim that it is sufficient to prove:

$$\sum_{j=1}^{n} x_j v_j \leq ||\mathbf{x}||_2 ||\mathbf{v}||_2.$$

for any nonzero vectors $\mathbf{x}$, $\mathbf{v} \in \mathbf{R}^n$. For if this is true, we may construct $\mathbf{v}$ by $v_j = \text{sign}(x_j)\text{sign}(y_j)y_j$ for any $\mathbf{y} \in \mathbf{R}^n$ and $j = 1, \ldots, n$ so that the Cauchy-Schwarz inequality is valid;

(iii) To prove the inequality in (ii), note that for *any* $\lambda \in \mathbf{R}$

$$0 \leq ||\mathbf{x} + \lambda \mathbf{v}||_2^2 = (\mathbf{x} + \lambda \mathbf{v})^{\mathsf{T}} (\mathbf{x} + \lambda \mathbf{v}),$$

so

$$2\lambda \sum_{j=1}^{n} |x_j v_j| \leq ||\mathbf{x}||_2 + \lambda^2 ||\mathbf{v}||_2.$$

Now ***select*** a specific $\lambda = ||\mathbf{x}||_2 / ||\mathbf{v}||_2$, simplifying the above inequality yields

$$2 \sum_{j=1}^{n} |x_j v_j| \leq 2 ||\mathbf{x}||_2 ||\mathbf{v}||_2,$$

which proves the inequality in (ii). Thus the Cauchy-Schwarz inequality is proved. □

A.2 Taylor's Theorem (In One Variable)

If $f \in C^n[a,b]$ and if $f^{(n+1)}$ exists on the open interval (a,b), then for any points c and x in the closed interval $[a,b]$,

$$f(x) = \sum_{k=0}^{n} \frac{1}{k!} f^{(k)}(c)(x-c)^k + E_n(x)$$

where, for some point ξ between c and x, the error term is

$$E_n(x) = \frac{1}{(n+1)!} f^{(n+1)}(\xi)(x-c)^{n+1}.$$

A.3 Taylor's Theorem (In Two Variables)

Let $f \in C^{n+1}([a,b] \times [c,d])$. If (x,y) and $(x+h, y+k)$ are points in the rectangle $[a,b] \times [c,d] \subseteq \boldsymbol{R}^2$, then

$$f(x+h, y+k) = \sum_{i=0}^{n} \frac{1}{i!} \left(h\frac{\partial}{\partial x} + k\frac{\partial}{\partial y} \right)^i f(x,y) + E_n(h,k)$$

where

$$E_n h, k) = \frac{1}{(n+1)!} \left(h\frac{\partial}{\partial x} + k\frac{\partial}{\partial y} \right)^{n+1} f(x+\theta h, y+\theta k)$$

in which θ lies between 0 and 1.

APPENDIX B
EXPERIMENTAL DATA

Appendix B reports all experimental data recorded during the course of this thesis. In order to get appropriate units (Pa/cm^2), all vectors should be multiplied by a factor of 4.893.

The normal loads used in all experiments are the set N.

N = [39.58 49.58 59.58 69.58 79.58 89.58]

A sled with a PMMA surface was used for the experiments presented in this thesis, however, data was also recorded for two alternate sled surfaces: bovine leather and aluminum, which will be used in future work.

The following are the averages of the data sets for each sled surface. For tables B.1-B.6, each column represents values for a particular normal load from N and each row contains average values under a particular speed (in mm/min) of testing.

Table B.1: Static friction using PMMA sled.

Speed	N_1	N_2	N_3	N_4	N_5	N_6
250	13.00	15.42	19.28	20.46	23.98	26.18
400	13.12	16.48	18.10	19.98	23.22	26.10
500	5.56	7.36	10.88	14.16	17.50	19.80
600	13.12	17.16	18.84	20.26	23.30	25.28
750	13.26	17.68	20.36	20.86	22.38	27.64
1000	13.36	15.28	17.92	20.16	22.44	24.72

Table B.2: Dynamic friction using PMMA sled.

Speed	N_1	N_2	N_3	N_4	N_5	N_6
250	11.228	13.8316	16.493	19.309	21.9642	24.5474
400	12.3318	15.0592	17.8862	20.496	23.0552	25.5642
500	3.5549	6.82728	10.0538	13.0432	16. 0848	19.1872
600	11.5672	14.1182	16.7200	19.3984	21.8200	24.2776
750	10.0630	12.1198	14.416	16.7884	19.3138	21.6528
1000	9.5609	11.7772	14.0432	16.2838	18.3808	20.6796

Table B.3: Static friction using bovine leather sled.

Speed	N_1	N_2	N_3	N_4	N_5	N_6
250	12.60	18.02	26.22	31.00	37.72	43.08
500	8.32	14.76	22.98	24.38	30.42	36.44
750	14.00	14.20	19.50	25.88	26.72	35.38
1000	10.48	17.36	23.24	26.22	36.36	39.08

Table B.4: Dynamic friction using bovine leather sled.

Speed	N_1	N_2	N_3	N_4	N_5	N_6
250	5.57482	10.1913	14.8918	19.8960	24.7438	30.0194
500	4.15808	8.26412	12.0498	16.9084	21.9142	26.0788
750	5.11758	9.20692	13.4586	17.7844	21.7406	26.1718
1000	4.95152	9.81974	14.224	18.7864	23.2618	27.4498

Table B.5: Static friction using aluminum sled.

Speed	N_1	N_2	N_3	N_4	N_5	N_6
250	17.98	21.78	24.34	27.92	30.38	35.00
500	14.18	17.36	19.76	24.26	23.96	27.76
750	27.66	31.42	33.50	36.74	39.62	41.26
1000	6.82	9.62	11.88	14.42	16.66	19.84

Table B.6: Dynamic friction using aluminum sled.

Speed	N_1	N_2	N_3	N_4	N_5	N_6
250	17.0218	20.5916	23.9466	27.3194	30.5928	33.7024
500	12.8314	15.6512	18.3482	21.0520	23.6258	26.3348
750	24.8498	28.1580	31.5374	34.6650	37.9722	41.1336
1000	3.82826	6.47072	9.35294	12.0524	14.7178	17.3518

APPENDIX C
PROGRAMS

All of the following programs are written for MATLAB.

C.1 Program for Computing C and n by Multiple Methods

The following program reads in data for friction force, F, and normal load, N, and using this data, computes C and n values for each of the three models presented in Chapter II. This program also plots C and n for static friction and dynamic friction against the speeds tested for each of the three models.

```
function speed_cnr(N, FS, FD)

clear all
format long

x_range=[250 400 600 750 1000];

%%%%%%%%%%%%%%%%%%%%%%%%%%%%%%%%%%%%%%%%%%%%%%%%%%%%

for j=1:2
   for i=1:5
        if j==1
                F=FS(i,:);
        else
                F=FD(i,:);
        end

        Y_data= log10(F);
```

```
        X_data= log10(N);

%%%%%%%% Linear fit

        N_bar = 1/(size(N,2))*sum(X_data);
        F_bar = 1/(size(N,2))*sum(Y_data);
        numlin = (X_data-N_bar)*(Y_data-F_bar)';
        denlin = (X_data-N_bar)*(X_data-N_bar)';
        n_l = numlin/denlin;
        log_cl = F_bar-(N_bar*n_l);
        c_l = 10^(log_cl);
        e_l = sum((Y_data-log10(c_l)-(n_l)*(X_data)).^2);

%%%%%%%%%%%% Quasi-Linear fit

        S = (F*F')*(F.^2*(Y_data.*X_data)') - (F.^2*Y_data')*(F.^2*X_data');
        T = (F*F')*(F.^2*(X_data.*X_data)') - (F.^2*X_data')^2;
        n_ql=S/T;
        Term1= F.^2*Y_data';
        Term2= n_ql*F.^2*X_data';
        Num=Term1 - Term2;
        Den = F*F';
        log_qc=Num/Den;
        c_ql=10^(log_qc);
        e_ql = (F.^2)*((Y_data-log10(c_ql)-(n_ql)*(X_data)).^2)';

%%%%%%%%%%% Nonlinear fit

        xdata = N;
```

```
        ydata = F;
        fun = inline('x(1)*(xdata.^x(2))','x','xdata');
        x = lsqcurvefit(fun,[1,2], xdata, ydata);
        c_nl = x(1);
        n_nl = x(2);
        e_nl = sum((ydata-(c_nl)*(xdata).^(n_nl)).^2);
        if j==1
                cs(i,:)=[c_l c_ql c_nl];
                ns(i,:)=[n_l n_ql n_nl];
        else
                cd(i,:)=[c_l c_ql c_nl];
                nd(i,:)=[n_l n_ql n_nl];
        end
    end
end

%% Linear plot

figure(1)
subplot(3,1,1)
plot(x_range, cs(:,1),x_range, cs(:,1),'ro')
hold on
plot(x_range, cd(:,1),'g--',x_range, cd(:,1),'r*')
ylabel('C')
title('Linear Model')
hold on
subplot(3,1,2)
plot(x_range, ns(:,1),x_range, ns(:,1),'ro')
hold on
```

```
plot(x_range, nd(:,1),'g--',x_range, nd(:,1),'r*')
ylabel('n')
subplot(3,1,3)
plot(x_range, cs(:,1)./ns(:,1),x_range, cs(:,1)./ns(:,1),'ro');
hold on
plot(x_range, cd(:,1)./nd(:,1),'g--',x_range, cd(:,1)./nd(:,1),'r*');
ylabel('R')
xlabel('Speed in mm/min')
print -deps fig_a.eps

%% Quasi-Linear plot

figure(2)
subplot(3,1,1)
plot(x_range, cs(:,2),x_range, cs(:,2),'ro')
hold on
plot(x_range, cd(:,2),'g--',x_range, cd(:,2),'r*')
ylabel('C')
title('Quasi-linear Model')
hold on
subplot(3,1,2)
plot(x_range, ns(:,2),x_range, ns(:,2),'ro')
hold on
plot(x_range, nd(:,2),'g--',x_range, nd(:,2),'r*')
ylabel('n')
subplot(3,1,3)
plot(x_range, cs(:,2)./ns(:,2),x_range, cs(:,2)./ns(:,2),'ro');
hold on
plot(x_range, cd(:,2)./nd(:,2),'g--',x_range, cd(:,2)./nd(:,2),'r*');
```

```
ylabel('R')
xlabel('Speed in mm/min')
print -deps fig_b.eps

%% Non-Linear plot

figure(3)
subplot(3,1,1)
plot(x_range, cs(:,3),x_range, cs(:,3),'ro')
hold on
plot(x_range, cd(:,3),'g--',x_range, cd(:,3),'r*')
ylabel('C')
title('Non-linear Model')
hold on
subplot(3,1,2)
plot(x_range, ns(:,3),x_range, ns(:,3),'ro')
hold on
plot(x_range, nd(:,3),'g--',x_range, nd(:,3),'r*')
ylabel('n')
subplot(3,1,3)
plot(x_range, cs(:,3)./ns(:,3),x_range, cs(:,3)./ns(:,3),'ro');
hold on
plot(x_range, cd(:,3)./nd(:,3),'g--',x_range, cd(:,3)./nd(:,3),'r*');
ylabel('R')
xlabel('Speed in mm/min')
print -deps fig_c.eps
```

C.2 A Simple GUI for the Linear Model

The second program allows the user to input friction force and normal load vectors, and then determines C and n values for the linear model as determined by equations (2.4) and (2.5). It graphs the base 10 logarithms of the inputted data against (2.2). This code creates the software presented in subsection 4.2.1.

```
clf
clear all

c=1;
n=1;


%action when 'plot' button is pressed
pltinit_callbk_str=...
   ['Y_data= log10(y_data);'...
    'X_data= log10(x);'...
    'N_bar = 1/(size(x,2))*sum(X_data);'...
    'F_bar = 1/(size(x,2))*sum(Y_data);'...
    'numlin = sum((X_data-N_bar).*(Y_data-F_bar));'...
    'denlin = sum((X_data-N_bar).*(X_data-N_bar));'...
    'n = numlin/denlin;'...
    'log_c1 = F_bar-(N_bar*n);'...
    'c = 10^(log_c1);'...
    'x=str2num(get(xrange,''string''));'...
    'y_data=str2num(get(yrange,''string''));'...
    'y=eval(get(fucfield,''string''));'];
```

```
%action when 'plot' button is pressed
pltlin_callbk_str=...
   ['Y_data= log10(y_data);'...
    'X_data= log10(x);'...
    'N_bar = 1/(size(x,2))*sum(X_data);'...
    'F_bar = 1/(size(x,2))*sum(Y_data);'...
    'numlin = sum((X_data-N_bar).*(Y_data-F_bar));'...
    'denlin = sum((X_data-N_bar).*(X_data-N_bar));'...
    'n_1 = numlin/denlin;'...
    'log_c1 = F_bar-(N_bar*n_1);'...
    'c_1 = 10^(log_c1);'...
    'c=c_1;'...
    'n=n_1;'...
    'x=str2num(get(xrange,''string''));'...
    'y_data=str2num(get(yrange,''string''));'...
    'y=eval(get(fucfield,''string''));'...
    '[i,k]=sort(X_data);'...
    'plot(X_data(k),y(k),X_data,Y_data,''ro'');'...
    'legend(''Linear'',''Data'');'...
    'xlabel(''log(N/A)'');'...
    'ylabel(''log(F/A)'');'...
    'cstring=num2str(c_1);'...
    'nstring=num2str(n_1);'...
    'gtext(''c='');'...
    'gtext(cstring);'...
    'gtext(''n='');'...
    'gtext(nstring);'];

%define the plot button
```

```
plotbutton=uicontrol('style','pushbutton',...
   'string','Linear', ...
   'fontsize',12, ...
   'position',[10,400,60,20], ...
   'callback', pltlin_callbk_str);

%define the initialize button
initbutton=uicontrol('style','pushbutton',...
   'string','initialize', ...
   'fontsize',12, ...
   'position',[475,400,75,20], ...
   'callback',pltinit_callbk_str);

%define the function editable text field
fucfield=uicontrol('style','text',...
   'string','log10(c)+ n*log10(x)', ..uicon
   'fontsize',12, ...
   'position',[420,1,0.0001,0.0001] ...
   );

x=1:.1:4;
xrange=uicontrol('style','edit',...
   'string','1:.1:4', ...
   'fontsize',12, ...
   'position',[110,1,100,20] ...
   );

%define some static text
uicontrol('style','text',...
```

```
   'string','Normal=',...
   'fontsize',12, ...
   'position',[40,1,60,20]);

y_data=1:.1:4;
yrange=uicontrol('style','edit',
   'string','1:.1:4', ...
   'fontsize',12, ...
   'position',[410,1,100,20] ...
   );

%define some static text
uicontrol('style','text',...
   'string','Friction=',...
   'fontsize',12, ...
   'position',[340,1,60,20]);
```

C.3 An Advanced GUI for Multiple Models

The final program allows the user to input friction force and normal load vectors, and then determines C and n values (for each of the three models) as in the first program, and with user inputted friction force and normal load vectors, it graphs the fitted equations against the actual data points. This code creates the software presented in subsection 4.2.2.

```
clf
clear all

c=1;
n=1;

%action when 'plot' button is pressed
pltinit_callbk_str=...
   ['Y_data= log10(y_data);'...
    'X_data= log10(x);'...
    'N_bar = 1/(size(x,2))*sum(X_data);'...
    'F_bar = 1/(size(x,2))*sum(Y_data);'...
    'numlin = sum((X_data-N_bar).*(Y_data-F_bar));'...
    'denlin = sum((X_data-N_bar).*(X_data-N_bar));'...
    'n = numlin/denlin;'...
    'log_cl = F_bar-(N_bar*n);'...
    'c = 10^(log_cl);'...
    'x=str2num(get(xrange,''string''));'...
    'y_data=str2num(get(yrange,''string''));'...
    'y=eval(get(fucfield,''string''));'];
```

```
%action when 'plot' button is pressed
pltlin_callbk_str=...
   ['Y_data= log10(y_data);'...
    'X_data= log10(x);'...
    'N_bar = 1/(size(x,2))*sum(X_data);'...
    'F_bar = 1/(size(x,2))*sum(Y_data);'...
    'numlin = sum((X_data-N_bar).*(Y_data-F_bar));'...
    'denlin = sum((X_data-N_bar).*(X_data-N_bar));'...
    'n_1 = numlin/denlin;'...
    'log_c1 = F_bar-(N_bar*n_1);'...
    'c_1 = 10^(log_c1);'...
    'c=c_1;'...
    'n=n_1;'...
    'x=str2num(get(xrange,''string''));'...
    'y_data=str2num(get(yrange,''string''));'...
    'y=eval(get(fucfield,''string''));'...
    '[i,k]=sort(x);'...
    'subplot(3,1,1);'...
    'plot(x(k),y(k),x,y_data,''ro'');'...
    'legend(''Linear'',''Data'');'...
    'axis([min(x) max(x) min(y_data) max(y_data)]);'...
    'cstring=num2str(c_1);'...
    'nstring=num2str(n_1);'...
    'gtext(''c='');'...
    'gtext(cstring);'...
    'gtext(''n='');'...
    'gtext(nstring);'];

%define the plot button
```

```
plotbutton=uicontrol('style','pushbutton',...
    'string','Linear', ...
    'fontsize',12, ...
    'position',[10,400,60,20], ...
    'callback', pltlin_callbk_str);


pltqlin_callbk_str= ...
    ['Y_data= log10(y_data);'...
     'X_data= log10(x);'...
     'A=sum(y_data.*y_data);'...
     'B=sum((y_data.^2).*(Y_data.*X_data));'...
     'C=sum((y_data.^2).*Y_data);'...
     'D=sum((y_data.^2).*X_data);'...
     'S=A*B-C*D;'...
     'E=A*sum((y_data.^2).*(X_data.*X_data));'...
     'T=E-sum((y_data.^2).*X_data)^2;'...
     'n_ql=S/T;'...
     'Term1= sum((y_data.^2).*Y_data);'...
     'Term2= n_ql*sum((y_data.^2).*X_data);'...
     'Num=Term1 - Term2;'...
     'log_qc=Num/A;'...
     'c_ql=10^(log_qc);'...
     'c=c_ql;'...
     'n=n_ql;'...
     'x=str2num(get(xrange,''string''));'...
     'y_data=str2num(get(yrange,''string''));'...
     'y=eval(get(fucfield,''string''));'...
     '[i,k]=sort(x);'...
     'subplot(3,1,2);'...
```

```
    'plot(x(k),y(k),x,y_data,''ro'');'...
    'legend(''Quasi-linear'',''Data'');'...
    'axis([min(x) max(x) min(y_data) max(y_data)]);'...
    'cstring=num2str(c_ql);'...
    'nstring=num2str(n_ql);'...
    'gtext(''c='');'...
    'gtext(cstring);'...
    'gtext(''n='');'...
    'gtext(nstring);'];

%define the plot button
plotbutton=uicontrol('style','pushbutton',...
   'string','Quasi-linear', ...
   'fontsize',12, ...
   'position',[80,400,100,20], ...
   'callback', pltqlin_callbk_str);

pltnlin_callbk_str=...
   ['xdata = x;'...
    'ydata = y_data;'...
    'fun = inline(''x(1)*(xdata.^x(2))'',''x'',''xdata'');'...
    'x_nl = lsqcurvefit(fun,[1,2], xdata, ydata);'...
    'c_nl = x_nl(1);'...
    'n_nl = x_nl(2);'...
    'c=c_nl;'...
    'n=n_nl;'...
    'x=str2num(get(xrange,''string''));'...
    'y_data=str2num(get(yrange,''string''));'...
    'y=eval(get(fucfield,''string''));'...
```

```
    '[i,k]=sort(x);'...
    'subplot(3,1,3);'...
    'plot(x(k),y(k),x,y_data,''ro'');'...
    'legend(''Non-linear'',''Data'');'...
    'axis([min(x) max(x) min(y_data) max(y_data)]);'...
    'cstring=num2str(c_nl);'...
    'nstring=num2str(n_nl);'...
    'gtext(''c='');'...
    'gtext(cstring);'...
    'gtext(''n='');'...
    'gtext(nstring);'];

%define the plot button
plotbutton=uicontrol('style','pushbutton',...
   'string','Non-linear', ...
   'fontsize',12, ...
   'position',[190,400,90,20], ...
   'callback', pltnlin_callbk_str);

%define the initialize button
initbutton=uicontrol('style','pushbutton',...
   'string','initialize', ...
   'fontsize',12, ...
   'position',[475,400,75,20], ...
   'callback',pltinit_callbk_str);

%define the function editable text field
fucfield=uicontrol('style','text',...
   'string','c*x.^n', ...uicon
```

```
   'fontsize',12, ...
   'position',[420,1,0.0001,0.0001] ...
   );

x=1:.1:4;
xrange=uicontrol('style','edit',...
   'string','1:.1:4', ...
   'fontsize',12, ...
   'position',[110,1,100,20] ...
   );

%define some static text
uicontrol('style','text',...
   'string','Normal=',...
   'fontsize',12, ...
   'position',[40,1,60,20]);

y_data=1:.1:4;
yrange=uicontrol('style','edit',...
   'string','1:.1:4', ...
   'fontsize',12, ...
   'position',[310,1,100,20] ...
   );

%define some static text
uicontrol('style','text',...
   'string','Friction=',...
   'fontsize',12, ...
   'position',[240,1,60,20]);
```

APPENDIX D

A RESEARCH PAPER

The following paper is a research paper that has been submitted for publication.

Frictional Study of Woven Fabric: Relationship Between Friction and Velocity of Testing[1]

D. Hermann,[2] S. S. Ramkumar* and P. Seshaiyer[2]

The Institute of Environmental and Human Health, Texas Tech University, Box 41163, Lubbock, TX 79409-1163, USA

Abstract

A simple friction factor has been devised to characterize the frictional properties of textile materials. The friction factor enables universal comparisons among different textile materials possible. A polymethyl methacrylate sled has been used as a standard friction substrate to characterize the friction of a woven cotton fabric. The influence of the velocity of testing on the frictional characteristics has been studied in detail using the novel friction factor. The present study elaborates the relationship between the speed of testing and the new fabric friction factor.

Keywords: friction factor, polymeric textiles, polymethyl methacrylate sled.

---

* To whom all correspondence should be sent [E-mail: s.ramkumar@ttu.edu]

[1] The friction factor used in the paper was originally conceived by Ramkumar

[2] Department of Mathematics and Statistics, Texas Tech University

Introduction

Most recently, a major upsurge in the research on the frictional characterization of polymeric textiles has taken place primarily due to the need for a standardized friction testing method [1-7]. Textile materials have known to deviate from the Amontons' law of friction [8-11]. This necessitates the evaluation of friction over a range of applied normal loads [1-7, 12]. Howell and Mazur's study of the fiber friction proved the deviations from Amontons' law [10]. Subsequent study by Wilson further proved the failure of Amontons' linear friction law in fabrics [8]. The importance of friction to the overall quality and the mechanical properties of solid polymers and textiles has been well researched and documented [13, 14, 15]. Briscoe and Tabor have emphasized the relationship between the friction and wear properties of polymers to their bulk properties [13]. Pierce stressed the importance of friction to the overall quality or the "hand" of fabrics but he did not endeavor to experimentally measure the frictional properties [15]. It is known that the frictional properties of textile materials depend on a number of testing parameters such as the applied normal load, area of testing, speed of testing and the nature of the contacting surfaces [8, 11, 16-19]. There is a plethora of literature available on the influence of applied normal loads and the area of testing on the frictional properties of textiles. However, there is a paucity of data on the influence of testing speeds on the frictional properties of textile materials. Nishimatsu and Sawaki have studied the effect of sliding speeds on the frictional property of pile fabrics and have observed a marginal decrease in the friction of fabrics with the increase in the velocity of testing [11]. Studies by Ajayi [16] and Virto and Naik [20] have shown that there is

limited influence of sliding speeds on the frictional properties. Most recently, Ramkumar et al. [21] have studied the effects of sliding speeds on the frictional properties of nonwoven fabrics. Results indicated that frictional resistance increased with an increase in the speed of testing. However, this study did not endeavor to examine the effect of sliding speeds on the frictional characteristics of a woven fabric. Woven fabrics are conventional and commodity textile products that are used in apparel goods. Therefore, it is necessary to evaluate the frictional properties of woven fabrics. Moreover, the influence of sliding speeds on the frictional properties of woven fabrics has to be evaluated due to the need for a standardized friction evaluation method.

The current study reports the results on the effect of different sliding velocities on the friction of a cotton woven fabric at different applied load levels. The sliding friction apparatus has been used to measure the friction over a range of applied normal loads. Previous studies have used this apparatus to obtain two friction values, the friction factor "*C*" and the friction index "n" [1-6, 16, 18]. More recently, Ramkumar et al. have used the sliding friction apparatus to derive a friction parameter "*K*" for characterizing the frictional properties of a set of 1×1 rib-knitted cotton fabrics [1]. This friction parameter *K* is mathematically logical and overcomes the difficulty that is associated with the common friction parameter "*C*." However, results from a most recent study have shown that characterizing the frictional properties using the friction parameter *K* is not practical and has led to the development of a refined friction factor, "*R*" [2]. The friction factor, *R*, has been used to characterize the frictional properties of enzyme treated fabrics. Enzyme treatment on fabrics etches the surface of the fabric enhancing the smoothness of fabrics.

The novel friction factor, R, obtained using the sliding friction method has been found to be an objective measure to characterize the enhancement in the smoothness of fabrics after enzyme treatment. The lower is the R value, the higher is the smoothness of the fabric and vice-versa [2]. However, the paper did not investigate the effect of speed of testing on the frictional properties and its effect on the new friction factor R. In another study, the refined friction factor, R, has been used to characterize the frictional properties of needle-punched nonwoven fabrics. The novel friction factor, R, was able to reflect subtle changes in the surface properties of needle-punched nonwovens [7, 21, 22]. This paper endeavors to study the relationship between the speed of testing and the new friction factor R.

Derivation of the New Friction Constant

As discussed in the introductory section of this paper, the coefficient of friction, μ, is not a logical measure to quantify the frictional properties of polymeric and textile materials. The friction force-normal load relationship is not a simple linear relationship [3, 4]. The friction force-normal load can be conveniently represented using Equation 1:

$$F / A = C(N / A)^n \tag{1}$$

where, F: Friction Force in Newtons;

N: Normal Load in Newtons;

A: Apparent Area in m^2;

C: Friction Parameter in Pascal^{1-n} and

n: Friction Index (non-dimensional).

Solving Equation 1 results in the values for the friction parameter, C, and the friction index, n. Experimental data for the static and dynamic frictional forces were obtained from the sliding friction tester as shown in Figure 1. Frictional forces were obtained at different applied normal loads and used in Equation 1. The friction parameter, C and friction index, n were used to obtain the composite friction factor, R.

$$C / n = R \tag{2}$$

where, C: Friction Parameter in Pascal^{1-n} ;

n: Friction Index (non-dimensional) and

R: Friction Factor in Pascal^{1-n}.

The composite friction factor, R has been used to examine the effect of sliding frictional speeds on the frictional properties of a woven cotton fabric. This factor will also enable us to understand the influence of different applied normal loads.

Experimental Method and Material

As the objective of the study was to examine the effect of sliding speeds on the frictional properties of textile materials, only one fabric has been used as the testing material. However, at each speed, frictional forces were evaluated at six different loads. The details of the fabric used are given in Table 1.

Friction Measurement

A sliding friction apparatus, as shown in Figure 1, has been used to measure the frictional forces over a range of applied normal loads. The sliding friction apparatus was

attached to a constant rate of extension tensile tester. The sliding friction apparatus consists of an aluminum platform on to which a frictionless pulley is attached. The maximum capacity of the load cell of the tensile tester was 25 kgf. The friction apparatus consists of a sled having an apparent contact area of 20 cm^2, consisting of a polymethyl methacrylate (PMMA) plate 10 mm in thickness mounted on a wooden block. One end of the sled was attached to the crosshead of the tensile tester by means of a nylon thread through a frictionless pulley as shown in Figure 1. Friction testing was carried out at six different applied normal loads. The minimum load used was 39.58 gms and the maximum load used was 89.58 gms. The load was incremented in steps of 10 grams. A rectangular piece of fabric was attached on the horizontal surface of the aluminum platform by a strip of double-sided adhesive tape. Special care was taken in ensuring no wrinkled samples were used, and that while attaching the sample to the tape no excessive pressure was applied. The sled, with the PMMA surface in direct contact with the fabric, was pulled across the sample, and the frictional data was recorded. For this study, the sled was always drawn across the weft (or filling) of the sample. Each test consisted of running the sled across the fabric using each of the six applied normal loads. Each test consisted of six runs corresponding to each applied normal load for a specified velocity. The study was conducted at five different velocities: 250 mm/min, 400 mm/min, 600 mm/min, 750 mm/min, and 1000 mm/min.

Data Collection and Friction Calculation

Both static and dynamic frictional resistances were measured for each run of a normal load at each sliding velocity. A built-in software in the tensile tester enables the automatic data recording and the calculation of static and dynamic friction force values. A Matlab program was written to solve Equations 1 and 2, and obtain the friction parameter values as given in Table 2.

Results and Discussion

The intent of this study was to understand the influence of testing sliding speeds on the friction values, C, n and R. As R is the composite friction factor that compounds the effects of the two friction indices, C and n, it was thought appropriate to investigate the effect of sliding speeds on R values. In addition, the study also investigated the adequacy of the power law relationship to represent the relationship between the friction force and the normal load. As is evident from Figure 2, the relationship between the friction force and the normal load can be conveniently represented by the power law relationship as represented in Equation 1. Furthermore, based on the residual values between the calculated and experimental values, it is evident that the power relationship is the best fit. Figure 3 delineates the effect of sliding speeds on the friction values. As is evident from the results, as speed of sliding increases, the sliding friction increases up to a certain speed level. There is a rapid increase in the sliding friction values with the increase in speed from 250 mm/min to 600 mm/min and then the effect gets flattened.

However in the case of dynamic friction, speed of sliding seems to have no significant effect.

Static friction is the initial friction offered to the smooth motion of the sled on the fabric. With increase in sliding speeds, the initial resistance to the movement is overcome with great momentum due to shearing of contact points resulting in enhanced friction. This may be the cause for the enhanced friction at sliding speeds from 250 mm/min to 600 mm/min. At lower sliding speeds, such as 250 mm/min to 600 mm/min, the time of contact between the fabric and the sliding friction sled is more resulting in more adhesion contact between the two surfaces. Since at lower sliding speeds, due to more adhesion, more force is required to overcome the adhesion, resulting in higher shearing at the contact points. The increased adhesion and the resultant shearing force results in a higher amount of friction. However, in the case of dynamic friction, which is the average of progressive resistances after the static resistance, the shearing forces do not rise with the speed resulting in very minimal change in friction values. However, with further increase in speed beyond 600 mm/min, there seems to be no significant change in friction. After certain levels of sliding speeds, the contact time between the sled and the fabric significantly reduce resulting in lower shearing forces at very high speeds resulting in marginal frictional variations. Changes in the frictional force values at different sliding speeds is clearly reflected in the friction factor values, C and R, as given by Table II. Results also show that both the friction parameter, C, and the friction factor, R, follow a similar trend with regard to sliding speed changes. This result clearly indicates that the composite factor, R, is a good quantitative factor to characterize the frictional properties.

There seems to be no significant change in the friction index, n, values with changes in sliding speeds. The friction index, n, characterizes the nature of the material and hence it is not influenced by the sliding speeds. Results obtained in this study clearly show that the friction factor, R, is quite adequate to quantify the frictional properties of polymeric textiles.

Conclusions

Frictional property of a cotton woven fabric at different sliding speeds has been objectively characterized using a novel composite friction factor. The composite friction factor was able to reflect the changes due to sliding speeds. Static friction increased steadily with the increase in the sliding speeds while there was no significant effect on dynamic friction values. Results also show that there is no significant effect on the friction index values due to the changes in the sliding speeds. In summary, the novel composite friction factor is a useful measure to characterize the frictional properties of polymeric textiles.

Acknowledgements

The work was funded in part by a contract from U.S. Army SBCCOM (contract # DAAD 13-00-C-0051 to its senior author Seshadri Ramkumar).

References

1. Ramkumar, S. S.; Leaf, G. A. V. and Harlock, S. C. J. Textile. Inst. 2000, 91, 374.

2. Ramkumar, S. S.. AATCC Review 2002, Vol. 2, 24.

3. Ramkumar, S. S. Indian J. Fiber and Textile Res. 2000, 25, 238.

4. Ramkumar, S. S. Method for Determining the Frictional Properties of Materials 2002, US Patent 6397672.

5. Ramkumar, S. S.; Wood, D. J., Fox, K. and Harlock, S. C. Textile Res. J., June 2003, 73(6), 469.

6. Ramkumar, S. S.; Wood, D. J., Fox, K. and Harlock, S. C. Textile Res. J., July 2003.

7. Rodel, C.; Ramkumar, S. S. Textile Res. J., 2003, 73(5), 381.

8. Wilson, D. J. Text. Inst. 1963, 54, 143.

9. Howell, H. G. J. Text. Inst. 1951, 42, 521.

10. Howell, H. G.; Mazur, J. J. Text. Inst. 1953, 44, 59.

11. Ohsawa, M.; Namiki, S. J. Text. Mach. Soc. Japan 1966, 19, 7 (Eng. Edn. 12, 143).

12. Ramkumar, S. S.; Shastri, L., Tock, R. W., Shelly, D.C., Smith, M. L., and Padmanabhan, S. J. Appl. Polymer Sci. 2003, 88, 2450.

13. Briscoe, B. J.; Tabor, D. Br. Polym. J. 1978, 10, 74.

14. Harlock, S. C.; Ramkumar, S. S. Textiles and the Information Society (Proceedings of the 78th World Conference of the Textile Institute) 1997, Vol. III, pp. 149.

15. Peirce, F. T. J. Text. Inst. 1930, 21, 377.

16. Ajayi, J. O. Text. Res. J. 1992, 62, 52.

17. Dreby, E. C. J. Res. Nat. Bur. Stand. 1943, 31, 237.

18. Carr, W. W.; Posey, J. E. and Tincher, W. C. Text. Res. J. 1988, 58, 129.

19. Clapp, T. G.; Timble, N. B. and Gupta, B. S. J. Appl. Polym. Sci. 1991, 47, 373.

20. Virto, L.; Naik, A. Textile Res. J. 1997, 67, 793.

21. Ramkumar, S. S.; Umrani, A. S., Parameswaran, S., Shelly, D.C., Tock, R. W. and Smith, M. L. Wear, (in print).

22. Ramkumar, S. S.; Roedel, C. J. Appl. Polym. Sci. 2003 (in print).

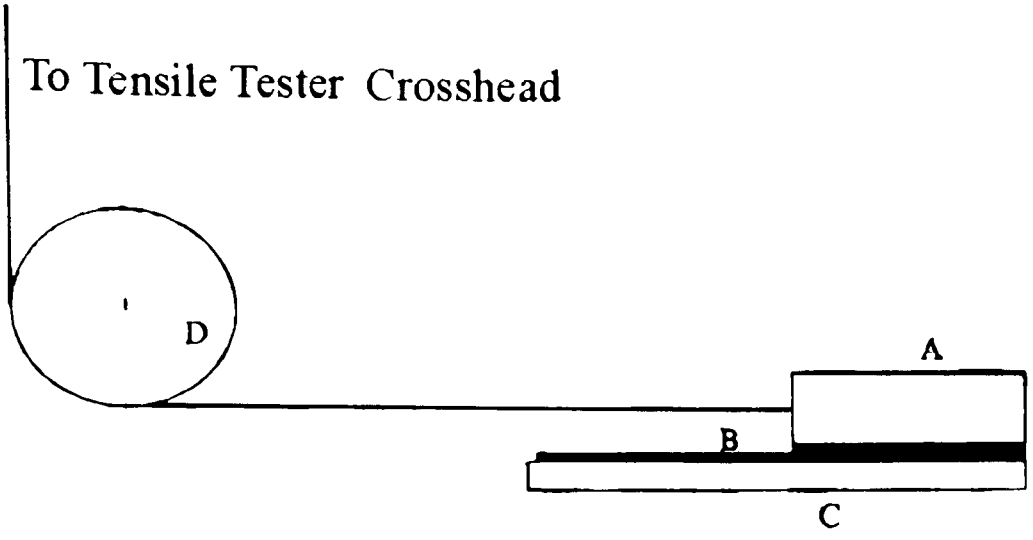

A: PMMA sled; B: fabric; C: aluminum platform; and D: frictionless pulley.

Figure 1: Schematic of the Sliding Friction Apparatus

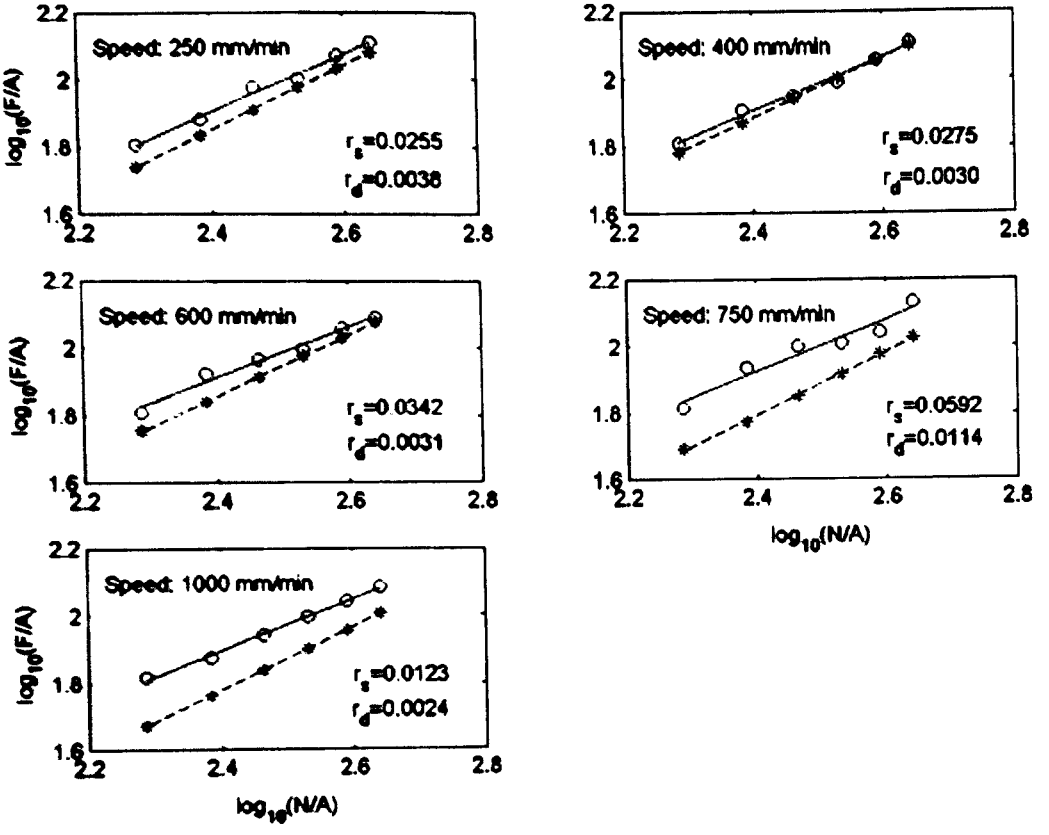

Figure 2: Log-log Relationship between Normal Load and Frictional Force. Static Experimental: circles; Static Computed: solid lines; Dynamic Experimental: asterisks; and Dynamic Computed: dashed lines. Here r_s and r_d denote the respective residual error between the experimental and computed values.

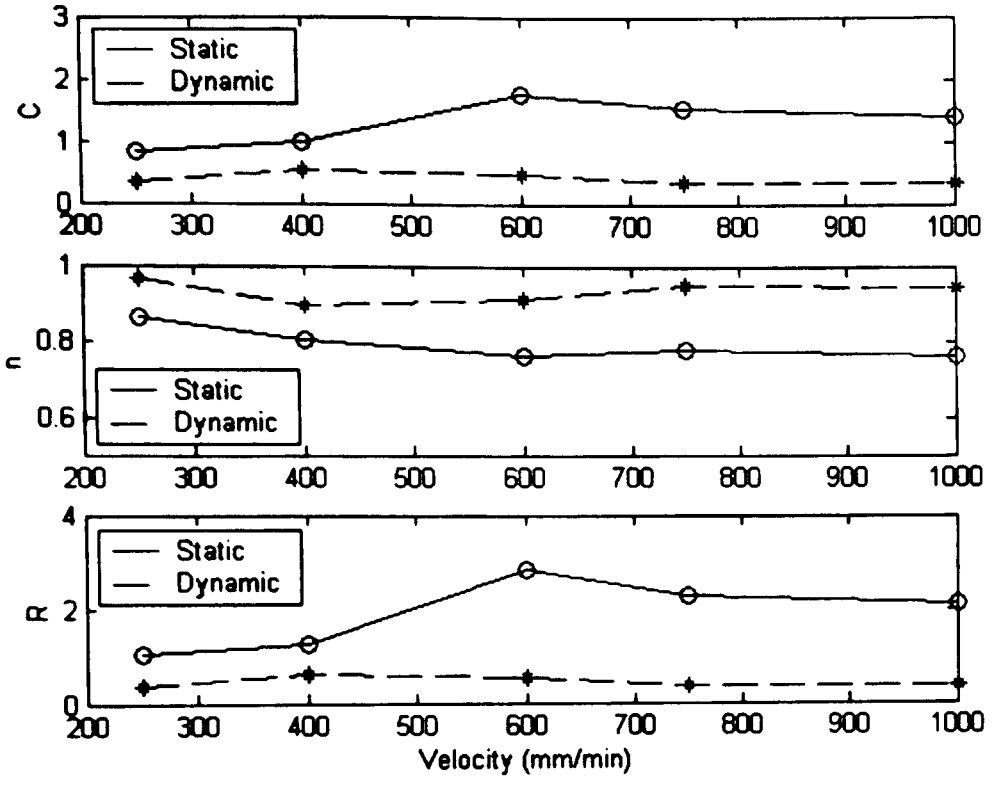

Figure 3: Relationship Between Friction Indices and Sliding Velocity

Table 1: Details of the Fabric Used

Type	Plain Woven Fabric
Ends/inch	98
Picks/inch	81
Warp count	38.3 Ne
Weft count	37.9 Ne
Weave	Plain
Weight	3.32 oz/sq.yd

Table 2: Experimental Results: Dynamic (D) friction and Static (S) friction

Velocity (mm/min)		C (Pa^{1-n})	n	R = C/n (Pa^{1-n})
250	S	0.815 (0.585)	0.867 (0.129)	1.044 (0.880)
	D	0.350 (0.112)	0.966 (0.040)	0.367 (0.135)
400	S	0.978 (0.284)	0.803 (0.060)	1.243 (0.433)
	D	0.547 (0.100)	0.896 (0.028)	0.614 (0.132)
600	S	1.750 (1.621)	0.595 (0.093)	2.845 (3.190)
	D	0.466 (0.060)	0.912 (0.021)	0.512 (0.078)
750	S	1.520 (1.030)	0.782 (0.191)	2.257 (1.764)
	D	0.332 (0.029)	0.947 (0.016)	0.351 (0.036)
1000	S	1.414 (1.028)	0.766 (0.134)	2.086 (1.840)
	D	0.328 (0.062)	0.944 (0.028)	0.349 (0.076)

Values within parentheses indicate standard deviation.

PERMISSION TO COPY

In presenting this thesis in partial fulfillment of the requirements for a master's degree at Texas Tech University or Texas Tech University Health Sciences Center, I agree that the Library and my major department shall make it freely available for research purposes. Permission to copy this thesis for scholarly purposes may be granted by the Director of the Library or my major professor. It is understood that any copying or publication of this thesis for financial gain shall not be allowed without my further written permission and that any user may be liable for copyright infringement.

Agree (Permission is granted.)

_____ _____

Student Signature Date

Disagree (Permission is not granted.)

_____ _____

Student Signature Date